

See discussions, stats, and author profiles for this publication at: <https://www.researchgate.net/publication/265387635>

Characterization of oxygen ion beams emitted from plasma focus

Article in *Vacuum* · December 2014

DOI: 10.1016/j.vacuum.2014.08.011

CITATIONS

2

READS

71

4 authors, including:



Sami Salo

Atomic Energy Commission of Syria

12 PUBLICATIONS 30 CITATIONS

SEE PROFILE



Sor Heoh Saw

Nilai University, Negeri Sembilan, Malaysia

98 PUBLICATIONS 909 CITATIONS

SEE PROFILE

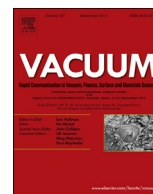


Sing Lee

INTI International University

393 PUBLICATIONS 3,540 CITATIONS

SEE PROFILE



Characterization of oxygen ion beams emitted from plasma focus



Mohamad Akel^{a,*}, Sami Alsheikh Salo^a, Sor Heoh Saw^{b,c}, Sing Lee^{b,c,d}

^a Department of Physics, Atomic Energy Commission, Damascus, P. O. Box 6091, Syria

^b INTI International University, 71800 Nilai, Malaysia

^c Institute for Plasma Focus Studies, 32 Oakpark Drive, Chadstone, VIC 3148, Australia

^d Physics Department, University of Malaya, Kuala Lumpur, Malaysia

ARTICLE INFO

Article history:

Received 2 June 2014

Received in revised form

11 August 2014

Accepted 13 August 2014

Available online 27 August 2014

Keywords:

Ion beam

Scaling law

Plasma focus

Lee model

Oxygen gas

ABSTRACT

The Lee model is modified to include oxygen in addition to other gases. It is then applied to characterize the ion beams emitted from the low energy plasma focus PF 1 kJ device operated with oxygen gas. The numerical experiments give the following results: ion fluence- 3×10^{18} ions m^{-2} , ion flux- 2.4×10^{26} ions $m^{-2} s^{-1}$, ion energy- 261 keV, ion number- 3.5×10^{13} , ion current- 3.5 kA, and damage factor- $1.12 \times 10^9 Wm^{-2} s^{0.5}$. Numerical experiments are systematically carried out on other plasma focus devices of various energies. Scaling trends are suggested for oxygen ion beam characteristics. These results provide much needed benchmark reference values and scaling trends for ion beams of a plasma focus operated in oxygen gas.

© 2014 Elsevier Ltd. All rights reserved.

1. Introduction

The plasma focus produces copious amounts of neutrons, highly energetic ions, relativistic electrons and X-rays. Energetic ions from the focus are used for processing thin films irradiated at different distances from the focus pinch [1]. The generated ion beams are of short time duration with continued and wide range of energies (few keV up to MeV). Ion implantation is a powerful technique used in research and industry for doping and modification of the surface of materials. The exposure of a material to such plasma environment leads to different effects and process such as amorphization, melting, fast cooling, and interaction with highly reactive plasma ions, sputtering, and deposition and so on. Although many works presented the observation of different topographic changes on plasma focus-treated surfaces, these topographic changes need more attention in order to understand the involved processes by correlating plasma focus parameters to different surface modifications [2–6]. On the other hand, the different properties of the deposited films are attributed to ion energy flux generated by plasma focus. Thus, ion energy flux and other ion beam characteristics play a key role to deposit smooth and uniform films of diverse properties [7–9]. Rico et al. studied the effects of oxygen

incorporation, by ion implanting, on the crystallization behavior of Strontium Bismuth Tantalate (SBT) thin films using a small plasma focus device with oxygen filling gas, and found that the incorporation of oxygen into the intermediate fluorite phase produces a better crystallization of the SBT perovskite phase, increasing the driving force for the fluorite-perovskite transformation. These preliminary results indicate that the implantation of oxygen by a plasma focus is a promising technique to lower the processing temperature of SBT thin films [10]. Rico et al. also reported the results of crystallization of amorphous zirconium thin films using ion beams generated by oxygen plasma focus. The oxygen-irradiated films showed a delayed and less extensive cubic nucleation, but a more ordered structure and well-defined grains [11]. We note that research on oxygen plasma focus concentrated on the treated surface modifications, but no results have been reported about the ion beam properties emitted from plasma focus leading to these changes. The correlation between the plasma focus parameters and produced ion beam properties could be of help to understand the plasma surface interactions and to find the optimum conditions for desired material science applications. The Lee model code [12,13] had been extended, based on the virtual plasma diode mechanism proposed by Gribkov et al. [14,15], for studying of ion beams from plasma focus [16,17]. In this work, we apply the code version RADPF5.15FIB, further extended to oxygen, to characterize the ion beams emitted from oxygen plasma focus at various conditions. We discuss in some detail the results of many numerical

* Corresponding author.

E-mail address: pscientific14@aec.org.sy (M. Akel).

experiments carried out using this modified code on different plasma focus devices.

2. Calculations of ion beam properties produced by plasma focus

S. Lee and Saw [17] derived the equation for the flux of the ion beam; linked to the Lee model code and hence computed the ion beam properties of the plasma focus for various gases. They proposed that since the ion beam exits the focus pinch as a narrow beam with little divergence, the exit beam is best characterized by the ion number per unit cross-section which we term the fluence. Following Lee and Saw we use the following equations:

$$\text{Flux (ions m}^{-2}\text{s}^{-1}) = J_b = 2.75 \times 10^{15} \left(f_e / [M Z_{\text{eff}}]^{1/2} \right) \times \left\{ (\ln[b/r_p]) / (r_p^2) \right\} (I_{\text{pinch}}^2) / U^{1/2} \quad (1)$$

$$\text{Fluence (ions m}^{-2}) = 2.75 \times 10^{15} \tau \left(f_e / [M Z_{\text{eff}}]^{1/2} \right) \times \left\{ (\ln[b/r_p]) / (r_p^2) \right\} (I_{\text{pinch}}^2) / U^{1/2} \quad (2)$$

where $M = 16$ for oxygen, cathode radius b ; and $f_e = 0.14$ (the fraction of energy converted from pinch inductive energy PIE into beam kinetic energy BKE) is equivalent to ion beam energy of 3%–6% E_0 for cases when the PIE holds 20%–40% of E_0 as observed for low inductance PF. The diode voltage U is $U = 3V_{\text{max}}$ taken from data fitting in extensive earlier numerical experiments [16,17], where V_{max} is the maximum induced voltage of the pre-pinch radial phase. The code is configured with the parameters of the experiment. The value of the ion flux is deduced by computing the values of effective charge Z_{eff} , pinch radius r_p , pinch duration τ , pinch current I_{pinch} and U . Once the flux is determined, the following quantities are also computed: power density flow (energy flux) (Wm^{-2}), current density (Am^{-2}), current (A), ions per sec (ions s^{-1}), fluence (ions m^{-2}), number of ions in beam (ions), energy in beam (J), damage Factor (is defined as energy flux \times (pulse duration) $^{0.5}$) ($\text{Wm}^{-2} \text{s}^{0.5}$), and energy of fast plasma stream (J).

3. Numerical experiments: results and discussions

3.1. Ion beam properties of PF 1 kJ operated with oxygen gas

The PF 1 kJ plasma focus device [10,11] operated with oxygen filling gas has been used for ion beam implantation and irradiation of different materials. In this work, we use the modified Lee model code, to get some information about the ion beams emitted from PF

1 kJ. To start the calculations, the modified Lee model code is configured to operate as the PF 1 kJ starting with the bank, tube and fitted parameters shown in Table 2 [18].

Then, for studying the effect of pressure on the ion beam characteristics, more numerical experiments were carried out; but varying oxygen gas pressure from 11 Pa to 120 Pa (see Table 1).

Table 1 shows that the ion energy decreases with increasing gas pressure from 307 keV to 55 keV, due to the induced voltage reduction in the radial phase with higher pressures. It can be noticed that the ion flux initially increases with the increase in gas pressure and reaches a maximum ($3.1 \times 10^{26} \text{ ions m}^{-2} \text{ s}^{-1}$) at a pressure of 67 Pa. The fluence has the same trend with pressure, and the peak value of the fluence is $6.2 \times 10^{18} \text{ ions m}^{-2}$ at oxygen gas of 93 Pa. The beam ion number increases with the increase in gas pressure until the plasma pinch becomes very weak. The beam ion number range from 2×10^{13} to 7.6×10^{13} for PF 1 kJ. Plasma focus devices have three typical regimes of influence of ion and plasma beams upon a target material placed downstream of the pinch [15,19,20]: (i) “implantation mode” of irradiation when power flow density of the streams is (10^9 – 10^{11} Wm^{-2}) (ii) screening of the surface by a secondary plasma cloud in the so-called “detachment mode” ($\approx 10^{11}$ – 10^{12} Wm^{-2}) (iii) strong damage with the absence of implantation in the “explosive destruction mode” ($\approx 10^{12}$ – 10^{14} Wm^{-2}). The numerical experiments show that maximum power flow density reaches $1 \times 10^{13} \text{ Wm}^{-2}$ at a pressure of 40 Pa, and decreases with higher pressures. So, based on the obtained power flow densities, it can be said that the explosive destruction mode is dominant for the PF 1 kJ operation. The damage factor is defined as power flow density multiplied by (pulse duration) $^{0.5}$. It is shown that, the damage factor reaches almost $1.2 \times 10^9 \text{ Wm}^{-2} \text{ s}^{0.5}$ for PF 1 kJ at a pressure of 40 Pa.

3.2. Ion beam characteristics for plasma focus devices with a range of energies

Numerical experiments were carried out systematically on plasma focus devices operated with oxygen (see Table 2). For each of these devices, model parameters were fitted and then used for the computation at various pressures. For each run the dynamics is computed by the code which also computes the ion beam properties (beam ion number, ion beam energy, flux, fluence, current, power flow density and damage factor).

In the same way as described for the PF 1 kJ we carried out numerical experiments for the range of different plasma devices (see Table 2) to obtain the trends across the range of plasma focus operated with oxygen filling gas. The results are shown in Table 3.

From Table 3, we see: (1) the I_{peak} and I_{pinch} typically decrease as E_0 is reduced; except for NX2, NX3 and PF1000 which produces higher performance in I_{peak} and I_{pinch} because of their unusually low L_0 . The values of I_{peak} and I_{pinch} for the other studied devices are relatively low due to larger L_0 . There is no evident trend with E_0 . (2)

Table 1
Variation of oxygen ion beam properties emitted from PF 1 kJ.

p_0 (Pa)	Ion fluence ($\times 10^{18} \text{ m}^{-2}$)	Ion flux ($\times 10^{26} \text{ m}^{-2} \text{ s}^{-1}$)	Ion energy (keV)	Ion number ($\times 10^{13}$)	Ion current (kA)	Power flow density ($\times 10^{12} \text{ Wm}^{-2}$)	Damage factor ($\times 10^9 \text{ Wm}^{-2} \text{ s}^{0.5}$)
11	1.5	1.5	307	2.0	2.7	7.6	0.75
13	1.8	1.7	300	2.3	2.9	8.3	0.84
27	3.0	2.4	261	3.5	3.5	10	1.12
40	4.2	2.8	224	4.4	3.7	10	1.2
67	5.8	3.1	158	5.9	3.6	7.7	1.1
93	6.2	2.5	104	7.0	3.1	4.2	0.66
107	5.6	1.9	78	7.3	2.7	2.4	0.41
120	4.2	1.2	55	7.6	2.2	1.1	0.2

Table 2
In the first column are displayed the plasma focus under consideration. The remaining columns are the energy of the bank E_0 , the anode and cathode radius a and b , the anode length z_0 , static inductance L_0 , capacitance C_0 , short-circuited resistance r_0 , charging voltage V_0 and model parameters f_m , f_{mr} and f_c , f_{cr} .

Device (ref.)	E_0 (kJ)	a (cm)	b (cm)	Z_0 (cm)	L_0 (nH)	C_0 (uF)	r_0 (m Ω)	V_0 (kV)	f_m	f_c	f_{mr}	f_{cr}
PF 400 J [21]	0.37	0.6	1.55	1.7	40	0.95	10	28	0.07	0.7	0.13	0.7
PF 1 kJ [18]	0.43	1.75	4.9	6.75	69	3.86	20	14.9	0.004	0.7	0.02	0.45
ICTP PFF [22]	2.2	0.95	3.2	16	102	30	24	12	0.06	0.7	0.15	0.7
PF 2.2 kJ [23]	2.2	1.05	4	12.5	330	7.1	62	25	0.01	0.7	0.15	0.7
APF [24]	2.6	1	2.235	14.8	145	36	8	12	0.02	0.7	0.15	0.7
NX2 PF [25]	2.7	1.9	4.1	5	20	28	2.3	14	0.06	0.7	0.16	0.7
AECS PF2 [18]	2.8	0.95	3.2	16	280	25	25	15	0.1	0.7	0.2	0.7
INTI PF [25]	3.4	0.95	3.2	16	110	30	12	15	0.06	0.7	0.16	0.7
NX3 PF [16]	20	3	5.6	14	47	100	2.3	20	0.1	0.7	0.26	0.7
PF1000 [14]	486	11.55	16	60	33	1332	6.3	27	0.14	0.7	0.35	0.7

The ratio I_{peak}/a ranges over 53–241 kA/cm with no perceptible trend with E_0 . Pinch length and pinch radius generally correlate with “ a ”. (3) The beam duration τ varies with “ a ” from 11 to 422 ns; the ratio τ/a has a range of 11.6–37 ns/cm (We note that points (2) and (3) agree with [26]). (4) The mean energy of the beam ion has a range of 100–1000 keV. (5) The ion fluence is $6 \times 10^{18} - 2.7 \times 10^{20}$ ions m^{-2} , has no correlation with E_0 . (6) The ion flux has a relatively bigger range of $2.5 \times 10^{19} - 6.5 \times 10^{20}$ ions $m^{-2} s^{-1}$ being greater for the smaller devices. (7) The energy fluence ranges over $1 \times 10^5 - 3.8 \times 10^7$ J m^{-2} . (8) The energy flux has a range $4.2 \times 10^{12} - 7.8 \times 10^{14}$ W m^{-2} . (9) The number of beam ions increases with E_0 having a value of 5×10^{13} for the 0.37 kJ PF 400 J and a greater value (4000 times) for the PF1000. (10) The beam energy at exit varies from 0.2% to 5.5% of E_0 . (11) The ion beam current

varies from 3.1 to 404 kA being 3.4%–21% of I_{peak} . (12) A damage factor (Table 3) is defined as energy flux \times (pulse duration) $^{0.5}$ with units of $Wm^{-2} s^{0.5}$. This factor ranges over $7 \times 10^8 - 1.7 \times 10^{11}$ $Wm^{-2} s^{0.5}$. (13) Post-pinch Fast plasma stream (FPS) energy at exit is estimated over the range of 2.8% and 14.5% of E_0 with speeds of 6–29 cm/ μs . (14) The plasma diode voltage varies from 15 to 153 kV and the impedance ranges from 0.13 to 0.6 Ω across the whole range of machines. (15) The azimuth magnetic field at the pinch's border ranges from 71 to 2694 kG. (16) The radius ratio ranges from 0.09 to 0.12 for all devices. The results are summarized in Table 4, which gives the range of the oxygen beam properties and the scaling suggested by an inspection of Table 3.

As an example we note that Table 4 has a range of ion number fluence from $3.4 \times 10^{19} - 2.7 \times 10^{20}$ ions m^{-2} a variation of 8

Table 3
A range of plasma focus and computed oxygen ion beam characteristics.

Device	PF 400 J	PF 1 kJ	ICTP	PF 2.2 kJ	APF	NX2	AECS PF2	INTI	NX3	PF1000
E_0 (kJ)	0.37	0.428	2.16	2.22	2.6	2.7	2.8	3.4	20	486
L_0 (nH)	40	69	102	330	145	20	280	110	47	33
V_0 (kV)	28	14.9	12	25	12	14	15	15	20	27
“ a ” (cm)	0.6	1.75	0.95	1.05	1	1.9	0.95	0.95	3	11.5
$c = b/a$	2.6	2.8	3.4	3.8	2.24	2.16	3.4	3.4	1.9	1.4
p_0 (Pa)	240	93	133	133	467	400	93	333	400	267
I_{peak} (kA)	127	92	141	91	157	412	114	195	723	2143
I_{peak}/a (kA/cm)	212	53	148	87	157	217	120	205	241	186
I_{pinch} (kA)	66	30	70	55	107	206	66	85	399	688
z_p (cm)	1.3	2.2	1.3	1.4	1.4	2.8	1.4	1.3	4.6	18.3
r_p (cm)	0.07	0.19	0.1	0.09	0.09	0.22	0.09	0.09	0.3	1.39
Radius ratio (r_p/a)	0.11	0.11	0.096	0.09	0.09	0.114	0.093	0.093	0.1	0.12
τ (ns)	13.6	24.8	12	14.6	13.3	32.1	11	13.6	48	422
τ/a (ns/cm)	22.7	14.2	12.63	13.9	13.3	16.9	11.6	14.3	16	36.7
V_{max} (kV)	12	5	11	10	18	25	13	12	51	30
$U = 3V_{max}$ (kV)	36	15	33	30	54	75	39	36	153	90
Diode imped. U/I_{pinch} (Ω)	0.54	0.5	0.47	0.54	0.5	0.36	0.6	0.42	0.38	0.13
Z_{eff}	7.3	6.9	7.1	6.6	6.8	6.8	7.1	6.7	6.7	5.2
Ion fluence ($\times 10^{20} m^{-2}$)	0.34	0.06	0.5	0.34	0.87	1.2	0.4	0.75	2.3	2.7
Ion flux ($\times 10^{27} m^{-2} s^{-1}$)	5.1	0.25	4	2.3	6.5	3.6	3.6	5.5	4.8	0.65
Mean ion energy (keV)	296	104	236	196	376	515	281	239	1030	470
En fluence ($\times 10^6 J m^{-2}$)	1.6	0.1	1.8	1.1	5.2	9.5	1.8	2.9	38	21
En flux ($\times 10^{13} Wm^{-2}$)	24	0.42	15	7.3	39	30	16	21	78	5
Ion number ($\times 10^{14}$)	0.5	0.7	1.2	1.1	2.4	17	0.99	2.1	67	2000
Ion number/kJ ($\times 10^{14}$)	1.35	1.64	0.55	0.5	0.8	6.3	0.35	0.62	3.35	4.11
IB energy (J)	2.4	4	5	4	14	139	4	8	1099	15,473
IB energy/kJ	6.5	9.34	2.31	1.8	5.4	51.5	1.43	2.35	55	32
IB energy (% E_0)	0.65	0.2	0.2	0.2	0.6	5.1	0.2	0.2	5.5	3.2
IB current (kA)	8.8	3.1	12	8.2	19.5	57	10.2	16.9	149	404.1
IB current (% I_{peak})	6.93	3.4	8.5	9	12.4	14	8.94	8.7	21	19
Beam power ($\times 10^9$ W)	0.36	0.05	0.4	0.24	1.1	4.3	0.4	0.6	23	37
Dam Fr ($\times 10^{10} Wm^{-2} s^{0.5}$)	2	0.07	1.6	0.9	4.5	5.3	1.7	2.4	17	3.2
Ion speed (cm/ μs)	188	111.2	168	153	212	248	184	169	351	237
Plasma stream En (J)	18	28	160	62	123	399	110	292	1950	37,845
Plasma stream En (% E_0)	4.9	6.5	7.4	2.8	4.8	14.5	3.9	8.6	9.7	7.8
PS speed (cm/ μs)	22	6	24	17	19	16	29	18	23	9
Mag. Field ($0.2I_{pinch}/r_p^2$) (kG)	2694	166	1400	1358	2642	851	1630	2100	886.7	71.2

Table 4

Summary: range of ion beam properties and likely scaling.

Property	Units (multiplier)	Range	Suggested scaling
Fluence	ions m ⁻² ($\times 10^{20}$)	0.06–2.7	Independent of E_0
Flux	ions m ⁻² s ⁻¹ ($\times 10^{27}$)	0.25–6.5	Independent of E_0
Mean ion energy	keV	104–1030	Independent of E_0
Energy fluence	J m ⁻² ($\times 10^6$)	0.1–38	Independent of E_0
Energy flux	W m ⁻² ($\times 10^{13}$)	0.42–78	Independent of E_0
Beam exit radius	Fraction of radius “a”	0.09–0.12	Independent of E_0
Beam ion number/kJ	ions per kJ ($\times 10^{14}$)	1.35–6.3	Independent of E_0
Beam energy	% of E_0	0.2–5.5	Independent of E_0
Beam energy/kJ	per kJ of E_0	1.4–55	Independent of E_0
Beam current (% I_{peak})	% of I_{peak}	3.4–21	Independent of E_0
Damage factor	($\times 10^{10}$ Wm ⁻² s ^{0.5})	0.07–17	Independent of E_0

through a huge range of E_0 from 0.4 to 486 kJ (except for PF 1 kJ the fluence is 6×10^{18} ions m⁻²). The variation is independent of E_0 on inspection of the numbers in Table 3. Table 4 suggests that $6 \times 10^{18} - 2.7 \times 10^{20}$ ions m⁻² may be set as a benchmark for the ion beam number fluence for oxygen operated Mather-type PF. We infer that the independence of E_0 of this fluence is related to the constancy of energy per unit mass. This energy density is the central scaling parameters of the PF for the whole range of machines from sub kJ to MJ [16,26]. The number of beam ions leaving the focus is found to vary from 2×10^{17} ions for the 500 kJ PF1000 to 5×10^{13} for the half kJ PF 400 J. There is a distinct correlation to E_0 , modified by a dependence on I_{peak} (or L_0). Table 4 suggests a benchmark of $1.35 \times 10^{14} - 6.3 \times 10^{14}$ beam ions per kJ for PF's with low L_0 of 20–70 nH, dropping to $3.5 \times 10^{13} - 8 \times 10^{13}$ beam ions per kJ for those with higher inductance. The ion current may be set as 3.4%–21% of I_{peak} . The machines discussed in this paper range widely not just in terms of stored energies but also in terms of characteristics such as large L_0 . With this method, FIB and FPS parameters may be computed for any Mather focus operating with oxygen gas. These numerical experiments place ion beam measurements on a firm footing, provide guidance for experiments, and a reliable basis for estimating effects on target materials.

4. Conclusion

Oxygen ion beam properties of plasma focus have been computed by the modified Lee model code. The ion beam characteristics of low energy plasma focus PF 1 kJ device have been studied versus operating pressure and different energy plasma focus devices. The number of beam ions exiting the pinch is found to range from 2×10^{17} ions for the 500 kJ PF1000 to 5×10^{13} for the 0.4 kJ PF 400 J with a strong correlation to E_0 (increases with E_0). However because the anode radius (hence pinch radius) also increases with E_0 , the results show that the fluence (ions per unit beam area) is practically independent of E_0 . The ion number fluence is $3.4 \times 10^{19} - 2.7 \times 10^{20}$ ions m⁻² varying by a factor of only 8 through the huge range of E_0 from 0.4 to 500 kJ; with no clear pattern on dependence on E_0 . The variation in fluence is more dependent on the static inductance L_0 typically being lower for the machines with higher L_0 . The ion flux (fluence per unit time) is further complicated by the dependence of pinch duration to E_0 and L_0 ; thus finally again showing no clear dependence on E_0 . The mean energy per ion is dependent on the accelerating fields which are related to the induced voltages caused by the imploding speeds of the current sheet. For neutron-optimized machines these speeds are independent of E_0 as are found by a study of optimized plasma focus machines [26]; and this independence is related to the near constancy of energy density per unit mass across the range of optimized plasma focus machines. Hence the mean energy per ion has no clear dependence E_0 ; rather may be

influenced more by operating voltage and current per unit radius of the device. Thus the energy fluence and flux also show no clear dependence on E_0 . The beam ion number per kJ and the beam energy per kJ are found to all fall within relatively narrow ranges influenced by L_0 with no clear dependence on E_0 . The beam current as a percentage of I_{peak} has an even smaller range over the whole range of devices. These ranges are useful guidelines for designing experiments and applications. The damage factor was found to be $7 \times 10^8 - 1.7 \times 10^{11}$ Wm⁻² s^{0.5} across the whole range of devices; with exceptionally low values for machines with high L_0 and low I_{peak}/a . It is worthwhile to note that the energy flux range from $4.2 \times 10^{12} - 7.8 \times 10^{14}$ Wm⁻² for all these devices (operated in their ‘optimised’ mode) as shown in Table 3 means that the explosive destruction mode [15,20] is dominant for the oxygen plasma focus. Finally, we believe that the Lee model could be a useful tool for characterization of the ion beams emitted from plasma focus, leading to selection of the suitable plasma focus parameters for desired material processing applications.

Acknowledgment

The authors would like to thank Director General of AECS, for encouragement and permanent support. They would also like to express many thanks to Miss Sheren Isamael, who collaborated going through all the numerical experiments using Lee Model. S H S and S L acknowledge INT-CPR-01-02-2012, FRGS/2/2013/SG02/INTI/01/1, and IAEA No: 16934 CRP F1.30.13. S L acknowledges UM.S/625/3/HIR/43, UMRG102/10AFR in the preparation of this paper.

References

- [1] Rawat RS, Aggarwal V, Hassan M, Lee P, Springham SV, Tan TL, et al. Appl Surf Sci 2008;255(5):2932.
- [2] Kelly H, Lepone A, Marquez A, Sadowski M, Baranowski J, Skladnik-Sadowska E. IEEE Trans Plasma Sci 1998;26(1):113.
- [3] Lepone A, Kelly H, Lamas D, Marquez A. Appl Surf Sci 1999;143(1–4):124.
- [4] Bhuyan H, Mohanty SR, Borthakur TK, Rawat RS. Indian J Pure Appl Phys 2001;39(11):698.
- [5] Sadowski M, Zebrowski J, Rydygier E, Kucinski J. Plasma Phys Control Fusion 1988;30(6):763.
- [6] Ahmad M, Al-Hawat Sh, Akel M. J Fusion Energy 2013;32(4):471.
- [7] Khan IA, Hassan M, Hussain T, Ahmad R, Zakaullah M, Rawat RS. Appl Surf Sci 2009;255(12):6132.
- [8] Hussain T, Ahmad R, Khan IA, Siddiqui J, Khalid N, Bhatti AS, et al. Nucl Instrum Methods Phys Res Sect B Beam Interact Mater Atoms 2009;267(5):768.
- [9] Jabbar S, Khan IA, Ahmad R, Zakaullah M, Pan JS. J Vac Sci Technol A 2009;27(2):381.
- [10] Rico L, Gomez BJ, Stachoiti M, Pellegrini N, Feugeas JN, de Sanctis O. Braz J Phys 2006;36(3B):1009.
- [11] Rico L, Gomez BJ, Feugeas JN, de Sanctis O. Appl Surf Sci 2007;254(1):193.
- [12] Lee S. Radiative dense plasma focus computation package: RADPF [Online]. Available: 2013., <http://www.plasmafocus.net/IPFS/modelpackage/File1RADPF.htm>, <http://www.intimal.edu.my/school/fas/UFLF>.
- [13] Lee S. J Fusion Energy 2014;33(4):319.
- [14] Gribkov VA, Banaszak A, Bienkowska B, Dubrovsky AV, Ivanova-Stanik I, Jakubowski L, et al. J Phys D Appl Phys 2007;40:3592.
- [15] Pimenov VN, Demina EV, Maslyayev SA, Ivanov LI, Gribkov VA, Dubrovsky AV, et al. Nukleonika 2008;53(3):111.
- [16] Lee S, Saw SH. Phys Plasmas 2012;19:112703.
- [17] Lee S, Saw SH. Phys Plasmas 2013;20:062702.
- [18] Akel M, Al-Hawat Sh, Saw SH, Lee S. J Fusion Energy 2010;29(3):223.
- [19] Gribkov VA, Pimenov, Ivanov LI, Dyomina EV, Maslyayev SA, Miklaszewski R, et al. J Phys D Appl Phys 2003;36(15):1817.
- [20] Pimenov VN, Maslyayev SA, Ivanov LI, Dyomina EV, Gribkov VA, Dubrovsky AV, et al. Nukleonika 2006;51(1):71.
- [21] Soto L, Silva P, Moreno J, Silvester G, Zambra M, Pavez C, et al. Braz J Phys 2004;34(4b):1814.
- [22] Elgarhy MAI. Plasma focus and its applications. M.Sc. thesis. Cairo, Egypt: Al-Azhar University; 2010.
- [23] Mohanty SR, Bhuyan H, Neog NK, Rout RK, Hotta E. Jpn J Appl Phys 2005;44(7A):5199.
- [24] Habibi M, Amrollahi R, Attaran M. J Fusion Energy 2009;28(1):130.
- [25] Saw SH, Lee PCK, Rawat RS, Lee S. IEEE Trans Plasma Sci 2009;37(7):1276.
- [26] Lee S, Serban A. IEEE Trans Plasma Sci 1996;24(3):1101.